

Thermal diffusivity and conductivity of $\text{Zr}_{1-x}\text{Y}_x\text{O}_{2-x/2}$ ($x = 0, 0.084$ and 0.179) single crystals

Rémy Mévrel^{a,*}, Jean-Claude Laizet^a, Alban Azzopardi^b, Bérangère Leclercq^a,
Martine Poulain^a, Odile Lavigne^a, Didier Demange^a

^aONERA BP 72, 92322 Chatillon Cedex, France

^bSnecma-Moteurs, Site Villaroche, YKOS, 77556 Moissy-Cramayel, France

Received 15 June 2003; received in revised form 17 October 2003; accepted 25 October 2003

Abstract

The thermal diffusivity of $\text{Zr}_{1-x}\text{Y}_x\text{O}_{2-x/2}$ ($x = 0, 0.086$ and 0.179) single crystals has been determined up to 1100°C with a laser flash method designed to minimize radiative transfer effects. The thermal conductivity of these materials can be satisfactorily described in the framework of the phonon theory, provided a minimum phonon mean free path is introduced. Both experimental results and a theoretical approach indicate that for this system, and in the composition range explored, the high temperature limit of the thermal conductivity does not depend on the constitutional point defect content. The point defects influence the decrease of the thermal conductivity at intermediate temperatures.

© 2003 Elsevier Ltd. All rights reserved.

Keywords: Single crystals; Thermal conductivity; Thermal properties; ZrO_2

1. Introduction

Zirconia ceramics constitute an important class of materials of technological and scientific importance, due to a wide range of useful properties such as high chemical stability, high toughness, fast ion conduction, low thermal conductivity, that render this group of materials particularly attractive for various applications:¹ electrochemical cells, biomedical implants, thermal barrier coatings. In these applications, zirconia is partially (or fully) stabilised with the addition of heterovalent cations, for example yttrium, rare-earth elements, Mg, Ca, etc. Pure ZrO_2 exhibits a monoclinic↔tetragonal phase transformation in the range $1180\text{--}1200^\circ\text{C}$ (on heating) and $1050\text{--}920^\circ\text{C}$ (on cooling).² This phase transformation is accompanied by a large volume change, which generally prevents the use of pure zirconia and explains why few studies have concerned dense monoclinic zirconia.

The objective of this investigation is to determine the variation with temperature of the thermal conductivity of undoped and yttria-stabilized zirconia single crystals. Strictly speaking, as for nickel superalloy “single crystals”, the phrase “single grain” would be more appropriate to designate these materials which may contain twins and/or coherent precipitates. However, we will keep the phrase “single crystal”, which is the one adopted previously by authors^{3–6} who investigated similar materials, provided by the same supplier (Zirmat Corp., North Billerica).

It is expected that these results will shed some light on the effect of point defects on the thermal conductivity of doped zirconias, a topic of scientific interest^{7,8} as well as of technological importance, in particular for designing thermal barrier coatings.^{9,10}

Few results have been reported on the thermal conductivity of zirconia single crystals. Youngblood et al.⁵ determined the thermal diffusivity of a set of zirconia single crystals partially and fully stabilised with yttria up to $1000\text{--}1200^\circ\text{C}$. The results show a marked increase of the thermal diffusivity above around 600°C , which is attributed by the authors to radiative heat transfer. More recently, Bisson et al.⁶ determined the room

* Corresponding author. Tel.: +33-1-467-34499; fax: +33-1-467-34164.

E-mail address: remy.mevrel@onera.fr (R. Mévrel).

temperature thermal conductivity of undoped and yttria-doped zirconia single crystals by photothermal microscopy. Their results show a clear decrease of the thermal conductivity as a function of yttria content up to 0.21 mol.YO_{1.5} above which value, the thermal conductivity increases, an effect attributed to a possible ordering of the point defects.

The thermal conductivity of polycrystalline yttria–zirconia materials has also been investigated by Hasselman et al.,¹¹ Raghavan et al.¹² (for nearly dense materials), and by a number of authors^{13–15} who studied porous coatings. Concerning undoped ZrO₂, to our knowledge, only Raghavan et al.¹² reported the thermal conductivity (between 100 and 800 °C) of an undoped polycrystalline zirconia obtained by sintering at 1150 °C.

In the present work, the thermal diffusivity of Zr_{1-x}Y_xO_{2-x/2} single crystals undoped ($x=0$) and doped with YO_{1.5} ($x=0.084$ and 0.179) has been determined by the laser-flash technique up to 1200 °C. The variations as a function of temperature and of x , derived from these diffusivity measurements, are discussed within the framework of the phonon theory of thermal conductivity.

2. Experimental

2.1. Materials

The single crystals investigated, supplied by Zirmat Corp. (North Billerica), were produced by skull melting crystal growth, a directional solidification process. Compositions and density are reported in Table 1.

2.1.1. Composition

Apart from hafnium, an element usually associated with zirconium, no element other than Zr, Y or O was detected by electron probe microanalysis (EPMA). The atomic fraction Hf/(Hf+Zr) determined by EPMA, amounts to less than 0.01 (Table 1).

2.1.2. Structure

It is often mentioned that the tetragonal to monoclinic transition in undoped zirconia is deleterious for the integrity of specimens. However, the single crystals studied in this work present no obvious crack. According to Ingel et al.,³ such single crystals are heavily twin-

ned materials (with no visible high-angle grain boundaries). These twins, which form on cooling, reduce the strains resulting from the shape change during the cubic/tetragonal and tetragonal/monoclinic transformations. As observed by transmission electron microscopy by Wunderlich et al.,⁴ the thickness of the twin lamellas is about 100–300 nm. In the present work, we checked by Raman spectroscopy that no zirconia phase other than monoclinic was present in the undoped zirconia materials. We noted an increased opacity after the first excursion to 1200 °C, as mentioned by Adams et al.² for similarly heat treated zirconia materials.

According to the supplier information and in agreement with Raman spectra recorded at Laboratoire de Dynamique, Interactions et Réactivité (LADIR, CNRS, Thiais, France), as well as published TEM observations by Martinez-Fernandez et al.,¹⁶ crystal B which corresponds to a partially stabilized zirconia is a mixture of tetragonal precipitates within a cubic matrix, and crystal C is fully cubic.

2.2. Diffusivity—laser flash technique

For measuring the thermal diffusivity, a single pulse (duration: 3–5 ms; energy: 5 J) from a CO₂ laser (wavelength: 10.6 μm) was directed on one face of a disc placed inside a high temperature furnace (atmosphere: argon). The incident laser pulse is absorbed at the surface of the zirconia-based materials, which have an absorption edge in the range 5–7 μm according to Cox et al.¹⁷ An HgCdTe infrared detector was used to measure the temperature from the rear face of the specimens over the 20–1200 °C range. An optical long-wave pass filter which eliminates the wavelengths shorter than 8 μm was interposed between the back face of the specimens and the detector. Thus, radiation coming from inside the zirconia material (which corresponds to wavelengths shorter than 7 μm) is stopped by the filter and the radiation recorded by the detector comes only from the back surface of the specimen. With this arrangement, no opaque coating is therefore needed on either face of the specimen, as employed in general for measuring the thermal diffusivity of semitransparent materials.

Diffusivity specimens consisted of 10 mm discs with thicknesses of 1.15 and 2.15 mm (ZrO₂), 2.17 mm ($x=0.084$) and 1.73 mm ($x=0.179$). The discs were

Table 1
Composition and density of the single crystals studied in the present work

Sample	Amount of YO _{1.5} (mol.%)	Amount of Y ₂ O ₃ (wt.%)	Hf/(Zr + Hf) at.%	Density (kg M ⁻³) present study	Theoretical density (kg M ⁻³)
A	0	0	1.0	5845 ± 4	5859
B	8.4	7.7	0.75	6043 ± 4	6053
C	17.9	16.6	1.0	5942 ± 8	5961

ultrasonically machined out of slices cut with a diamond wheel, perpendicularly to the crystal growth axis. Specimen surfaces were ground with SiC abrasive papers down to a 1200 grit.

The variations of back-surface temperature as a function of time (called thermograms in what follows) are analyzed by a method¹⁸ which takes into account radiation and convection losses, and these loss terms are determined essentially by considering the cooling part of the experimental thermogram. The thermal diffusivity, α , is then calculated by minimizing the difference between a calculated thermogram and the experimental one, this optimizing operation being carried out on the rising temperature part (usually between $t_{\min}=0.6 t_{1/2}$ and $t_{\max}=1.5 t_{1/2}$, with $t_{1/2}$ the time at mid-height).¹⁹ With this data treatment, a diffusivity value can be calculated for each time step in the interval between t_{\min} and t_{\max} . This provides an indication of the reliability of the results since, for a homogeneous material, this calculated diffusivity should be constant in this interval.

Each value of diffusivity reported represents the average value of 4–6 measurements.

2.3. Thermal conductivity

The thermal conductivity was calculated according to:

$$K = \alpha \cdot \rho \cdot C_p \quad (1)$$

where α is the thermal diffusivity ($\text{m}^2 \text{s}^{-1}$), ρ the density (kg m^{-3}) and C_p the specific heat capacity ($\text{J kg}^{-1} \text{K}^{-1}$).

2.4. Density

Density was determined by helium pycnometry (Accupyc 1330, Micromeritics, USA) and the values, reported in Table 1, show a good agreement with theoretical densities calculated from crystallographic data, indicating that the materials are fully dense.

For ZrO_2 , the theoretical density has been calculated from the unit cell dimensions derived in the study reported by Hill and Cranswick²⁰ on a high purity monoclinic ZrO_2 ($a=0.5146 \text{ nm}$; $b=0.5212 \text{ nm}$; $c=0.5313 \text{ nm}$; $\beta=99.22^\circ$) and by taking into account that the material studied in the present work contained some hafnium. It was also assumed that the introduction of hafnium ($\text{Hf}/(\text{Zr} + \text{Hf})=1.0 \text{ at.}\%$) did not affect the unit cell dimensions, given the close ionic radii of Hf^{4+} and Zr^{4+} (respectively 0.083 and 0.084 nm for a coordination number of 8).²¹ The density thus derived is 5859 kg m^{-3} , which is very close to the value measured in the present study (5845 kg m^{-3}).

The theoretical density of the yttria-containing zirconia single crystals were determined from the cell dimensions determined by Scott²² and by taking into account the hafnium content.

To calculate the density change with temperature, we adopted the thermal expansion coefficients determined experimentally by Adams² ($8.1 \times 10^{-6} \text{ K}^{-1}$ for pure zirconia) and those proposed by Kisi et al.²³ for cubic yttria-stabilized zirconia, derived from the crystallographic data determined by Terreblanche,²⁴ i.e. $10.5 \times 10^{-6} \text{ K}^{-1}$, a value which is practically independent of the yttria content and also close to the thermal expansion coefficient of the tetragonal phase.²⁵

2.5. Specific heat capacity

For the specific heat capacity of undoped zirconia, the reference data reported by NIST²⁶ have been used. To convert the molar specific values into specific heat capacity per unit mass, the hafnium content has been taken into account. For the specific heat capacity of yttria-zirconia systems, the values determined by Leclercq⁷ on $\text{Zr}_{1-x}\text{Y}_x\text{O}_{2-x/2}$ ($x=0.086$ and $x=0.152$) have been adopted. Although the composition of the zirconia richest in yttria does not exactly coincide with the material studied in the present work (respectively, $x=0.152$ and $x=0.179$), these values have been adopted for, as it can be seen in Fig. 1, the specific heat capacity of yttria-zirconia systems does not depend significantly on the yttria content in this range of concentration. This fact had also been shown at low temperature, between 15 and 300 K for $x=0.177$ and $x=0.204$ by Tojo et al.²⁷

The uncertainties are estimated to be less than 5% for the heat capacity, 5% for the diffusivity and 0.5% for the density, so the precision on the absolute value of the thermal conductivity is estimated at around 10%. It should be noted though that the measurements are done in similar conditions and the relative precision may be significantly less than this value.

3. Results

3.1. Thermal diffusivity

The variations in temperature of the thermal diffusivity of undoped ZrO_2 , reported in Fig. 2, show a very small scatter of the data points for two different specimens (differing by their thickness) and for two successive runs on each specimen.

Similarly, a remarkably small scatter of the results can be noticed in Fig. 3 for slightly different operating conditions (laser pulse duration of 3 and 5 ms) for yttria-containing single crystals (only one specimen of each composition has been studied).

The thermal diffusivity continuously decreases in temperature (Figs. 2 and 3). The experimental device employed in the present study appears to eliminate radiative heat transfer effect which, according to Youngblood et al.,⁵ causes an increase above 600°C in

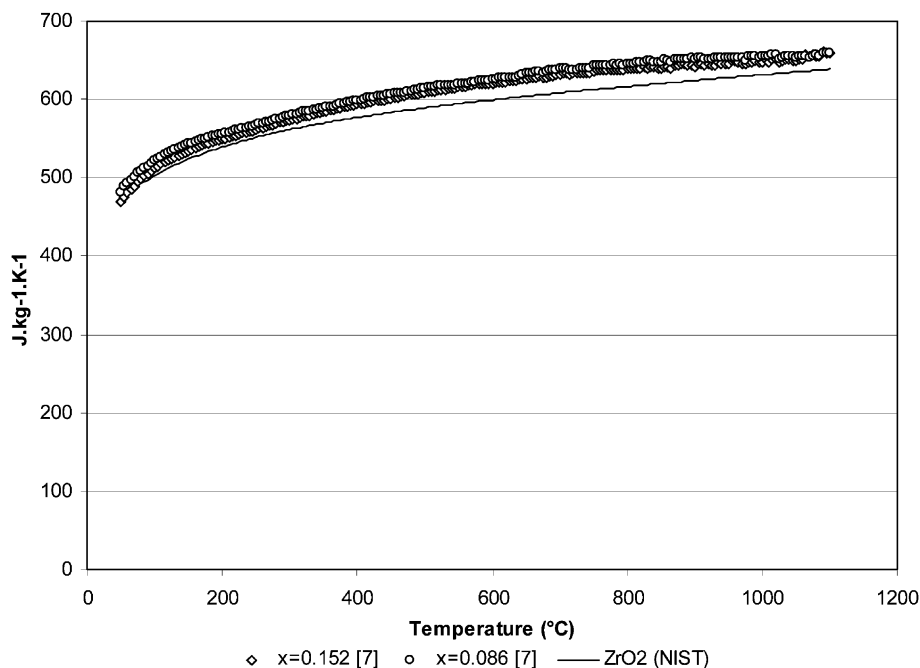


Fig. 1. Specific heat capacity of undoped zirconia and yttria-zirconia. See comments in text.

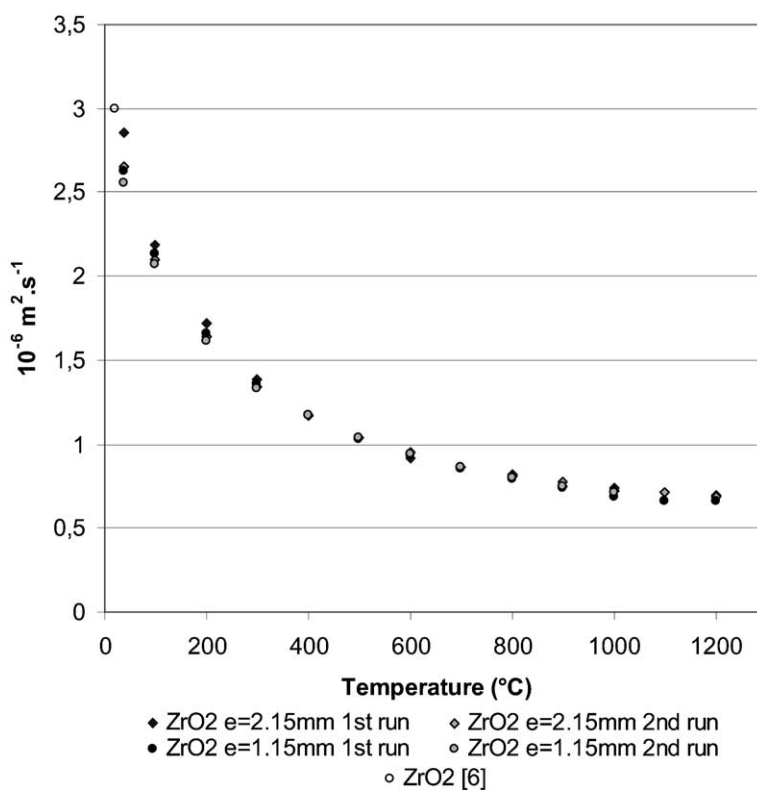


Fig. 2. Thermal diffusivity of undoped ZrO_2 single crystals. Each point is the average of at least four measurements at a given temperature.

the thermal diffusivity they recorded for zirconia single crystals containing yttria.

We note that the thermal diffusivity values obtained at room temperature on similar single crystals by Bisson et al.⁶ are in the continuation of the variations observed in the present work for the undoped zirconia and the

yttria-poor composition. For the yttria-rich composition, the room temperature value seems slightly high but the results are compatible if we take into account the experimental uncertainties (the experimental methods are different and the uncertainty reported by Bisson et al.⁶ is of the order of 15%).

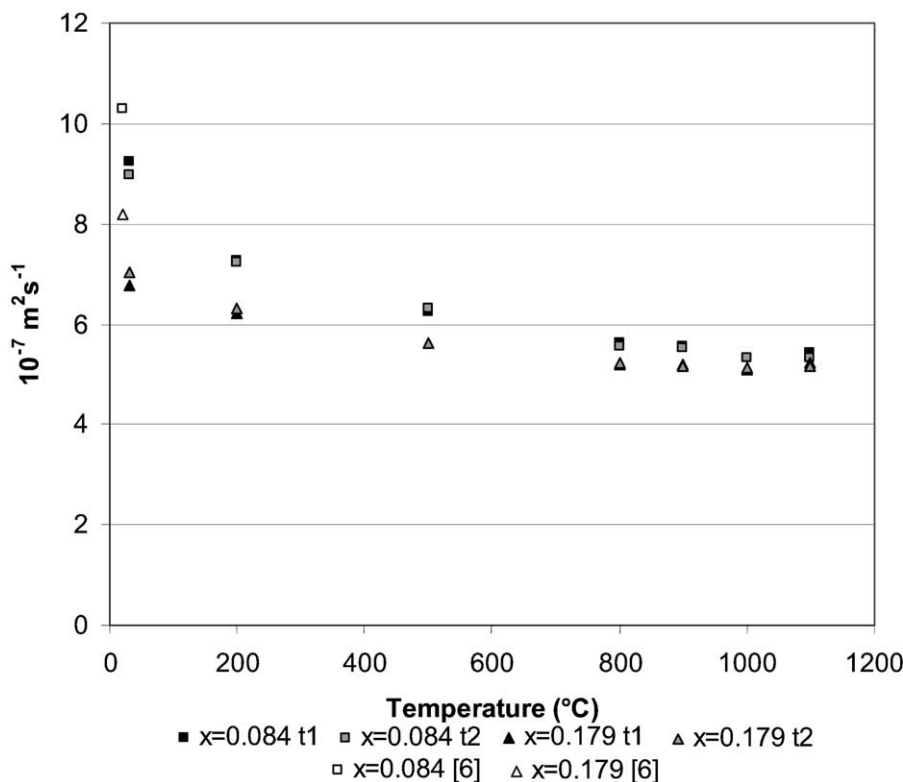


Fig. 3. Thermal diffusivity of $Zr_{1-x}Y_xO_{2-x/2}$ ($x = 0.084, 0.179$). Each closed symbol corresponds to the average of four measurements for a given set of conditions. For each composition, two laser pulse durations ($t_1 = 3$ ms and $t_2 = 5$ ms) have been used in the laser flash experiment. These results indicate a very good reproducibility.

3.2. Thermal conductivity

Fig. 4 shows the variations of the thermal conductivity in temperature. In this graph, for each composition, one point corresponds to the average of the thermal diffusivity of the different runs.

The thermal conductivity of ZrO_2 single crystals decreases in temperature, with a classical trend for ceramic materials, whereas for yttria-stabilized zirconias, the variations are much less pronounced. For the yttria-rich composition, above 200 °C, the thermal conductivity is constant within experimental error. At high temperature, we note that the thermal conductivities seem to converge towards a same value, for all the single crystals studied.

Given the experimental uncertainties, the results near room temperature are consistent with the values reported by Bisson et al.⁶ for single crystal zirconia, but determined by a completely different technique (infrared thermography).

Regarding undoped zirconia, if the thermal conductivity values at 100 and 200 °C coincide with the values reported by Raghavan et al.¹² for polycrystalline materials, we note that the temperature variations are different: in the present work, the thermal conductivity decreases more rapidly than the values for the polycrystalline materials. It is difficult to explain this

discrepancy. A priori, one would expect a polycrystalline material to have a lower thermal conductivity than a single crystal having the same composition. Moreover, according to Raghavan et al.,¹² the influence of the grain size on yttria-containing zirconia should be small, even for the small grain materials they studied (grain size > 100 nm). Another effect which would explain the difference is the presence of cracks in the single crystals. But the porosity of the single crystals is very low (< 1%) and the presence of cracks would also affect the room temperature values, which they do not. Moreover, at high temperature, the thermal conductivity of the gas inside the cracks would increase and this would result in values in excess of the values reported by Raghavan et al.,¹² contrarily to what is observed. Another effect to consider is the anisotropic structure of pure zirconia, which is monoclinic. In principle, the thermal conductivity is anisotropic for such a structure. This might result in different values of thermal conductivity for single crystals and for polycrystalline materials. However, it is to note that such a discrepancy would be independent of temperature (at least to the first order) whereas it increases as the temperature increases. We note also that Bisson et al.⁶ found no evidence of anisotropy for the thermal conductivity of a ZrO_2 single crystal by exploring different faces and different directions on one face of ZrO_2 single crystals.

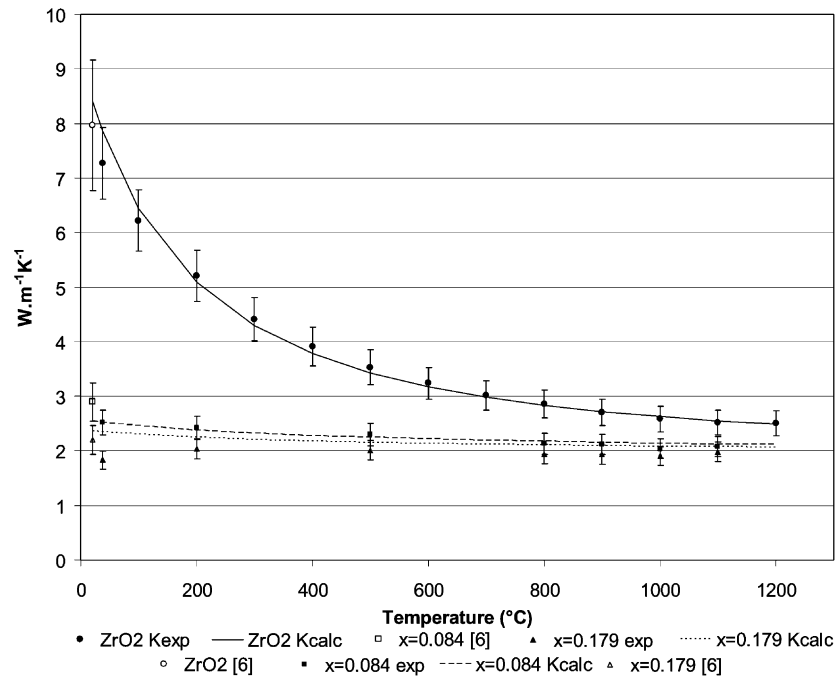


Fig. 4. Thermal conductivity as a function of temperature for $\text{Zr}_{1-x}\text{Y}_x\text{O}_{2-x/2}$ single crystals. The dark symbols (K_{exp}) are experimental values obtained in the present work and the open symbols refer to experimental values determined by infrared thermography.⁶ The continuous lines (K_{calc}) correspond to Eqs. (10) and (19) with the following values of the adjustable parameters: $A = 2400 \text{ W/m}$, $T_1 = 420 \text{ K}$ and $\beta = 1.5 \text{ K s}^{-2}$ (see text for details).

The thermal conductivity values of the yttria-stabilized zirconia single crystals are comparable with the values already reported by Raghavan et al.¹² In the present work, at low temperature, a decreasing trend is observed for $x = 0.084$, this does not seem to be the case for the polycrystal having the same composition. For $x = 0.179$, the value at room temperature is lower than the value at 200 and 500 °C. This would be consistent with previous results reported by Cahill et al.²⁸ for the thermal conductivity of yttria zirconia ($x = 0.15$) below room temperature where a glass-like behaviour can be observed.

4. Discussion

4.1. Lattice thermal conductivity

The lattice contribution of the thermal conductivity can be written as:²⁹

$$K = \frac{1}{3} \int_0^{\omega_{\max}} C'(\omega, T) \cdot v(\omega) \cdot l(\omega, T) d\omega \quad (2)$$

where $C'(\omega)d\omega$ is the contribution to the specific heat of the vibration modes having a frequency comprised between ω and $\omega + d\omega$, $v(\omega)$ is the phonon velocity ($= v$ constant in what follows) and $l(\omega, T)$ is the phonon mean free path.

In the framework of the Debye approach, ω_{\max} is Debye frequency ω_D , v can be considered constant and

equal to the sound velocity. Moreover, at temperature higher than the Debye temperature Θ_D , $C'(\omega)$ is proportional to ω^2 and independent from temperature:

$$C'(\omega, T) = B \cdot \omega^2$$

with B a constant.

Lastly, the mean free path $l(\omega)$ can be written as:

$$\frac{1}{l(\omega)} = \frac{1}{l_U(\omega)} + \frac{1}{l_P(\omega)} \quad (3)$$

where $l_U(\omega)$ is the mean free path associated with Umklapp phonon–phonon interactions and $l_P(\omega)$ is the mean free path for phonon–point defect interactions. This relationship assumes that the interaction mechanisms can be considered independent. These individual mean free paths can be expressed as:³⁰

$$\frac{1}{l_U(\omega)} = \frac{\omega^2 T}{D_U} \quad (4)$$

$$\frac{1}{l_P(\omega)} = \frac{c_d \omega^4}{D_P} \quad (5)$$

where D_U and D_P are parameters independent of temperature and frequency, c_d is the point defect concentration. In the following discussion, this concentration is defined as the ratio of the number of point defects and the total number of atomic sites.

4.2. Case 1: undoped zirconia

In the case of a solid containing no point defects, l_p can be neglected and the integration of expression (2) leads to the classical T^{-1} variations of the intrinsic thermal conductivity in the high temperature limit:³¹

$$K_{\text{int}} = \frac{1}{3} \int_0^{\omega_D} C'(\omega) \cdot v \cdot l(\omega, T) d\omega = \frac{1}{3} \int_0^{\omega_D} B\omega^2 v \cdot \frac{D_U}{\omega^2 T} d\omega = \frac{A}{T} \quad (6)$$

with

$$A = \frac{1}{3} Bv \cdot D_U \omega_D.$$

Theoretical approaches^{29,32} developed for solids having one atom per primitive cell give:

$$A = \frac{B'}{(2\pi)^3} M \cdot \Omega^{1/3} k_B^3 \Theta_D^3 / \hbar^3 \gamma^2 \quad (7)$$

where M is the atom mass, Ω is the atomic volume, γ is Grüneisen constant and Θ_D is Debye temperature. The value proposed by Klemens²⁹ for the numerical factor ($B' = 1.61$), based on a number of simplifying assumptions, usually gives a satisfactory description of the measured conductivity at high temperature.

To generalise these approaches to the case of solids containing p (> 1) atoms per unit cell, i.e. with optical branches in the phonon spectrum, Slack³³ finds that the result must be divided by $p^{2/3}$.

We note that the integrand in (6) being independent of ω , the contribution of all modes are important for the thermal conductivity at high temperature, even long wavelength phonons.

In fact, as for a number of other solids, the thermal conductivity of undoped zirconia decreases less rapidly than T^{-1} . This arises from the fact that $l(T)$ decreases with increasing temperature, but it cannot be shorter than the wavelength of the corresponding phonon, and this wavelength cannot, in turn, be much shorter than the distance between two neighbouring atoms.³⁴

To take this limit into account, we can introduce (as originally suggested by Roufosse and Klemens³⁵) a minimum mean free path l_{\min} such that:

$$l(\omega) = \frac{D_U}{\omega^2 T} \quad \text{if} \quad \frac{D_U}{\omega^2 T} > l_{\min} \quad (8)$$

$$l(\omega) = l_{\min} \quad \text{if} \quad \frac{D_U}{\omega^2 T} < l_{\min} \quad (9)$$

The integration of expression (2) gives:

$$K_{\text{int}} = \frac{1}{3} \int_0^{\omega'} B\omega^2 v \cdot \frac{D_U}{\omega^2 T} d\omega + \frac{1}{3} \int_{\omega'}^{\omega_D} B\omega^2 v \cdot l_{\min} d\omega = \frac{A}{T} \left[\frac{2}{3} \sqrt{\frac{T_1}{T}} + \frac{T}{3T_1} \right] \quad (10)$$

where

$$\omega' = \sqrt{\frac{D_U}{l_{\min} T}} = \sqrt{\frac{T_1}{T}} \omega_D \quad \text{and} \quad T_1 = \frac{D_U}{l_{\min} \cdot (\omega_D)^2} \quad (11)$$

Given all the simplifying assumptions underlying this model, we consider A and T_1 as adjustable parameters and the fit reported on Fig. 4 corresponds to $A = 2400 \text{ W m}^{-1}$ and $T_1 = 420 \text{ K}$.

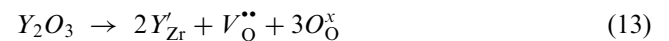
Bisson et al.⁶ have estimated $D_U = 2.9 \cdot 10^{+20}$ (S.I. units) for pure ZrO_2 . Given a Debye temperature³⁶ of 510 K,

$$l_{\min} = \frac{D_U}{T_1 \cdot (\omega_D)^2} = 0.15 \text{ nm} \quad (12)$$

which is of the same order of magnitude as the shortest interatomic distances in zirconia. In monoclinic zirconia, each zirconium ion is seven-fold coordinated, with Zr–O distances ranging from 0.205 to 0.228 nm.

4.3. Case 2: $\text{Zr}_{1-x}\text{Y}_x\text{O}_{2-x/2}$ ($x \neq 0$)

The approach exposed above can be extended to the case of zirconia–yttria systems. In these systems, the substitution of two zirconium ions by two yttrium ions is accompanied by the incorporation of one oxygen vacancy to keep the electroneutrality of the lattice according to the relation:



where, in terms of the Kroger–Vink notation, Y'_{Zr} designates an yttrium ion occupying a zirconium ion site (single negative charge), $V_{\text{O}}^{\bullet\bullet}$ is a doubly charged (positive) oxygen vacancy and O_{O}^x is an oxygen ion on an oxygen site (neutral). The electric charges are defined with respect to the pure zirconia lattice.

Two types of point defect are therefore introduced, yttrium ions (concentration c_Y) and oxygen vacancies (concentration $c_V = c_Y/2$), and the collisions of phonons with these defects are characterised by parameters D_{PY} and D_{PV} , respectively. The phonon mean path can be written as:

$$\frac{1}{l(\omega)} = \frac{1}{l_U(\omega)} + \frac{1}{l_P(\omega)} = \frac{\omega^2 T}{D_U} + \frac{c_Y \omega^4}{D_{PY}} + \frac{c_V \omega^4}{D_{PV}} = \frac{\omega^2 T}{D_U} + \left(\frac{c_Y}{D_{PY}} + \frac{c_V}{D_{PV}} \right) \omega^4 \quad (14)$$

For a composition $\text{Zr}_{1-x}\text{Y}_x\text{O}_{2-x/2}$, $c_Y = x/3$ and $c_V = x/6$, and the general expression for the mean free path can be rewritten as:

$$\frac{1}{l(\omega)} = \frac{\omega^2 T}{D_U} + \frac{c_d \omega^4}{D_P} \quad (15)$$

where $c_d = x/2$ is the concentration of point defects and

$$\frac{1}{D_P} = \frac{2}{3D_{PY}} + \frac{1}{3D_{PV}} \quad (16)$$

Introducing the minimum mean free path l_{\min} , Eqs. (8) and (9) can be rewritten as:

$$\frac{1}{l(\omega)} = \frac{\omega^2 T}{D_U} + \frac{c_d \omega^4}{D_P} \quad \text{if} \quad \frac{\omega^2 T}{D_U} + \frac{c_d \omega^4}{D_P} < \frac{1}{l_{\min}} \quad (17)$$

$$\frac{1}{l(\omega)} = \frac{1}{l_{\min}} \quad \text{if} \quad \frac{\omega^2 T}{D_U} + \frac{c_d \omega^4}{D_P} > \frac{1}{l_{\min}} \quad (18)$$

The integration of Eq. (2) is straightforward and gives:

$$\begin{aligned} K &= \frac{1}{3} \int_0^{\omega_1} B \omega^2 v \cdot \frac{1}{\frac{\omega^2 T}{D_U} + \frac{c_d \omega^4}{D_P}} d\omega \\ &\quad + \frac{1}{3} \int_{\omega_1}^{\omega_D} B \omega^2 v \cdot l_{\min} d\omega \\ &= \frac{A}{T} \frac{\omega_1}{\omega_D} \left(\frac{\omega_0}{\omega_1} \right) \arctg \left(\frac{\omega_1}{\omega_0} \right) + \frac{A}{3T} \frac{1}{1 + \left(\frac{\omega_1}{\omega_0} \right)^2} \\ &\quad \times \left[\left(\frac{\omega_D}{\omega_1} \right)^2 - \frac{\omega_1}{\omega_D} \right] \end{aligned} \quad (19)$$

with $\omega_0 = \sqrt{\frac{\beta T}{c_d}}$, $\beta = \frac{D_P}{D_U}$ and

$$\omega_1 = \omega_0 \sqrt{-\frac{1}{2} + \sqrt{\frac{1}{4} + \left(\frac{\omega'}{\omega_0} \right)^2}}$$

The frequency ω_1 is defined by $l(\omega_1) = l_{\min}$.

Only one more adjustable parameter has been introduced, β , and with $\beta = 1.5 \text{ K s}^{-2}$, a reasonable fit can be obtained for the variations as a function of temperature of the thermal conductivity of the yttria–zirconia systems studied (Fig. 4).

It has been implicitly assumed that the constants A and T_1 are the same for doped and undoped materials. This is certainly valid for low defect concentrations. For high concentrations, the quantity A in particular should be in principle re-evaluated as several quantities in Eq. (7) are dependent on composition. In particular, as underlined by Grimvall,³⁴ A varies as $M^{-1/2}$ given the mass dependence in Θ_D (which varies as $M^{-3/2}$). However, for the yttria–zirconia system, we do not expect

this term to vary much as the atomic masses of yttrium and zirconium are close (respectively, 88.91 and 91.22 g). The situation could be different if another dopant is considered.

According to the approach proposed, the value of the high temperature limit of the thermal conductivity for this system is given by $A/(3 \cdot T_1)$. The point defects present decrease the thermal conductivity at a given temperature but do not influence the high temperature limit of the thermal conductivity. This is because the limit is governed by value of the minimum mean free path, which has been assumed identical for undoped zirconia and yttria-stabilized zirconia. It is interesting to note that the limit calculated in the present work— $A/(3 \cdot T_1) = 1.9 \text{ W m}^{-1} \text{ K}^{-1}$ —is very close to the value determined theoretically by Slack³⁷ for the minimum thermal conductivity of zirconia ($2.06 \text{ W m}^{-1} \text{ K}^{-1}$), a value derived by remarking that the minimum mean free path of a phonon in a crystal must be of the order of one phonon wavelength.

5. Conclusion

The thermal diffusivity of $\text{Zr}_{1-x}\text{Y}_x\text{O}_{2-x/2}$ ($x=0, 0.086$, and 0.179) single crystals has been determined with a laser flash method. The use of a CO_2 laser and the interposition of a long wavelength-pass filter between rear face and detector minimized possible radiative effects. The thermal conductivity of these materials can be described in the framework of the phonon theory, if a minimum phonon mean free path is introduced. Both the experimental results and the theoretical approach indicate that for this system, and in the composition range explored, the high temperature limit for the phonon thermal conductivity does not depend on the defect content.

Acknowledgements

This work has been done in part within the program of international collaboration between the National Science Foundation (DMR-0099695) and the European Commission (GRD2-200-30211). Mathieu Fèvre is gratefully acknowledged for relevant remarks concerning the manuscript.

References

1. Kisi, E., Zirconia engineering ceramics. In *Key Engineering Materials*. Transtech Publications, 1998, pp. 153–154.
2. Adams, J. W., Nakamura, H. H., Ingel, R. P. and Rice, R. W., Thermal expansion behavior of single-crystal zirconia. *J. Am. Ceram. Soc.*, 1985, **68**(9), C228–C231.

3. Ingel, R. P., Willging, P. A., Bender, B. A. and Coyle, T. M., The physical and thermomechanical properties of monoclinic single crystals. In *Advances in Ceramics*, vol. 24A: *Science and Technology of Zirconia III*, ed. S. Somiya, N. Yamamoto and H. Yanagida. The American Ceramic Society, 1988, pp. 459–469.
4. Wunderlich, W. and R  hle, M., Critical stresses for microcracking in monoclinic zirconia. In *Advances in Ceramics*, vol. 24A: *Science and Technology of Zirconia III*, ed. S. Somiya, N. Yamamoto and H. Yanagida. The American Ceramic Society, 1988, pp. 509–515.
5. Youngblood, G. E., Rice, R. W. and Ingel, R. I., Thermal diffusivity of partially and fully stabilized (yttria) zirconia single crystals. *J. Am. Ceram. Soc.*, 1988, **71**(4), 255–260.
6. Bisson, J.-F., Fournier, D., Poulain, M., Lavigne, O. and M  vrel, R., Thermal conductivity of yttria-zirconia single crystals determined with spatially resolved infrared thermography. *J. Am. Ceram. Soc.*, 2000, **83**(8), 1993–1998.
7. Leclercq, B., Etude de la conductivit   thermique de mat  riaux    base de zircone. Doctorate thesis, University of Limoges, France, 2002.
8. Schelling, P. and Phillpot, S. R., Mechanisms of thermal transport in zirconia and yttria-stabilized zirconia by molecular-dynamics simulation. *J. Am. Ceram. Soc.*, 2001, **84**(12), 2997–3007.
9. Arnault, V., M  vrel, R., Alp  rine, S. and Jaslier, Y., Thermal barrier coatings for aircraft turbine airfoils: thermal challenge and materials. *La Revue de M  tallurgie-Science et G  nie des Mat  riaux*, 1999, **5**, 585–597.
10. Clarke, D. R., Materials selection guidelines for low thermal conductivity thermal barrier coatings. *Surf. and Coat. Technol.*, 2003, **163–164**, 67–74.
11. Hasselman, D. P. H., Johnson, L. F., Benten, H. D., Syed, R., Lee, H. M. and Swain, M. V., Thermal diffusivity and conductivity of dense polycrystalline ZrO_2 ceramics: a survey. *Am. Ceram. Soc. Bull.*, 1987, **66**(5), 799–806.
12. Raghavan, S., Wang, H., Dinwiddie, R. B., Porter, W. D. and Mayo, M. J., The effect of grain size, porosity, and yttria content on the thermal conductivity of nanocrystalline zirconia. *Scripta Mat.*, 1998, **39**(8), 1119–1125.
13. Brandt, R., Pawlowski, L., Neuer, G. and Fauchais, P., Specific heat and thermal conductivity of plasma sprayed yttria-stabilized zirconia and NiAl, NiCr, NiCrAl, NiCrAlY, NiCoCrAlY coatings. *High Temperatures-High Pressures*, 1986, **18**, 65–77.
14. Wilkes, K.E. & Lagedrost, J.F., Thermophysical properties of plasma sprayed coatings, NASA CR-121144 (1973).
15. Morrel, P. and Taylor, R., Thermal diffusivity of thermal barrier coatings of ZrO_2 stabilised with Y_2O_3 . *High Temperatures-High Pressures*, 1985, **17**, 79–88.
16. Martinez-Fernandez, J., Jimenez-Melendo, M. and Domingo-Rodr  guez, A., Microstructural evolution and stability of tetragonal precipitates in Y_2O_3 partially stabilized ZrO_2 single crystals. *Acta Metall. Mater.*, 1995, **43**(2), 593–601.
17. Cox, J. A., Greenlaw, D., Terry, G., McHenry, K. and Fielder, L., Comparative study of advanced IR transmissive materials. *SPIE*, 1986, **263**, 49–62.
18. Demange, D., Mesure de la diffusivit   thermique des composites 2D et 3D, des couches minces et des liquides par la m  thode flash. *La Revue de M  tallurgie-Science et G  nie des Mat  riaux*, 1999, **5**, 649–666.
19. Parker, W. J., Jenkins, R. J., Butler, C. P. and Abbott, G. L., Flash method of determining thermal diffusivity, heat capacity, and thermal conductivity. *J. Appl. Physics*, 1961, **32**(9), 1679–1684.
20. Hill, R. J. and Cranswick, L. M. D., International Union of Crystallography Commission on powder diffraction rietveld refinement round robin. II Analysis of Monoclinic ZrO_2 . *J. Appl. Cryst.*, 1994, **27**, 802–844.
21. Shannon, R. D., Revised effective ionic radii and systematic studies of interatomic distances in halides and chalcogenides. *Acta Cryst.*, 1976, **A32**, 751.
22. Scott, H. G., Phase relationships in the zirconia–yttria system. *J. Mat. Sci.*, 1975, **10**(9), 1527–1535.
23. Kisi, E. H. and Howard, C. J., Crystal structure of zirconia phases and their interrelation. *Key Engng Materials*, 1999, **153–154**, 1–35.
24. Terreblanche, S. P., *J. Appl. Cryst.*, 1989, **22**, 283.
25. Schubert, H., Anisotropic thermal expansion coefficients of Y_2O_3 -stabilized tetragonal zirconia. *J. Am. Ceram. Soc.*, 1986, **69**(3), 270–271.
26. Chase, M. W. Jr., NIST-JANAF Thermochemical Tables, Fourth Edition. *J. Phys. Chem. Ref. Data. Monograph*, 1998, **9**, 1–1951 Available on <http://webbook.nist.gov/>.
27. Tojo, T., Atake, T., Mori, T. and Yamamura, H., Excess heat capacity in yttria stabilized zirconia. *J. Thermal Anal. and Calorimetry*, 1999, **57**, 447–458.
28. Cahill, D. G., <http://users.mrl.uiuc.edu/cahill/tcdata/tcdata.html>. See also Fig. 6 in Cahill D.G., Watson S.K. & Pohl R.O., Lower limit to the thermal conductivity of disordered materials. *Phys. Rev.*, 1992, **B46** (10), 6131–6140.
29. Klemens, P. G., Theory of the thermal conductivity of solids. In *Thermal Conductivity*, ed. R. P. Tye. Academic Press, New York, 1969, pp. 1–68.
30. Klemens, P. G., The scattering of low-frequency waves by static imperfections. *Proc. Phys. Soc.*, 1955, 1113–1128.
31. Kittel, C., *Introduction to Solid State Physics*, 5th ed. J Wiley, UK, 1976.
32. Julian, C. L., Theory of heat conduction in rare-gas crystals. *Phys. Rev.*, 1965, **137**, A128–A137.
33. Slack, G. A., The thermal conductivity of nonmetallic crystals. *Solid State Physics*, 1979, **34**, 1–71.
34. Grimvall, G., *Thermophysical Properties of Materials*, 1999.
35. Roufousse, M. and Klemens, P. G., Thermal conductivity of complex dielectric crystals. *Phys. Rev. B: Condens. Matter*, 1973, **7**(12), 5379–5386.
36. Shirakami, T., Tojo, T., Ataka, T., Mori, T. and Yamamura, H., Low temperature heat capacities of zirconia and yttria-doped zirconia $(ZrO_2)_{1-x}(Y_2O_3)_x$ ($x=0, 0.02, 0.0396$). *Thermochimica Acta*, 1995, **267**, 415–420.
37. Slack, G. A., The thermal conductivity of nonmetallic crystals. *Solid State Physics*, 1979, **34**, 1–71 (see Table XVIII).